

Received March 1, 2020, accepted March 19, 2020, date of publication March 31, 2020, date of current version April 20, 2020.

Digital Object Identifier 10.1109/ACCESS.2020.2984523

Cooperative Guidance Considering Detection Configuration Against Target With a Decoy

SHAOBO WANG¹, YANG GUO^{1,2}, SHICHENG WANG¹, ZHIGUO LIU¹, AND SHUAI ZHANG¹

¹Department of Control, Xi'an Research Institute of High-Technology, Xi'an 710025, China

²College of Automation, Northwestern Polytechnical University, Xi'an 710072, China

Corresponding author: Yang Guo (guoyang820@foxmail.com)


This work was supported in part by the National Natural Science Foundation (NNSF) of China under Grant 61673386, and in part by the China Postdoctoral Science Foundation under Grant 2017M613201 and Grant 2019T120944.

ABSTRACT We consider the scenario where two pursuers are required to intercept an enemy evader that launches a decoy. Under the assumption that all four aircrafts have first-order linear dynamic characteristics, a cooperative guidance law is designed in two stages: the unidentified decoy stage and the discriminated decoy stage. In the unidentified decoy stage, the predictive guidance law is designed based on the method of the highest probability interval (HPI). This guidance law can maximize the probability of intercepting the real target despite the decoy's presence, thus providing an interception maneuver advantage for later cooperative guidance to the real target. In the discriminated decoy stage, based on the optimal control theory, an optimal guidance law considering the detection configuration is designed, which reduces the estimation error in the detection process and improves the interception performance. Simulation results verify the feasibility of the phased cooperative guidance law.

INDEX TERMS Cooperative guidance, predictive guidance, highest probability interval, optimal control, detection configuration, estimation error.

I. INTRODUCTION

In recent years, the use of multiple interceptors (pursuers) to target maneuvering evaders has been widely studied. These studies involve the design of a guidance law and the estimation of a target state. For designing the guidance law, optimal control theory [1], [2], theory of differential game [3], and sliding mode control [4] have been employed. However, earlier studies have designed the guidance law on the premise that the motion of the maneuvering target is known. Therefore, a number of studies were conducted where the state of target is estimated in real time in the guidance process. The methods for estimating the target state is often designed with the implementation of the Kalman filter [5], [6]; some examples are the extended Kalman filter [7], multiple model adaptive filtering [8], and interactive multiple model filtering [9]. These filter based techniques, in combination with the aforementioned control methods, for designing the guidance law are all based on the separation theorem (ST) [10]. The separation theorem states that the controller and estimator of linear Gaussian system can be designed independently.

The associate editor coordinating the review of this manuscript and approving it for publication was Mohsin Jamil .

However, for nonlinear non-Gaussian systems, the separation theorem cannot be proved to be effective. To solve this problem, some scholars proposed the method of generalized separation theorem (GST) [11]. In addition, during the interception of the target using multi-aircraft, the geometric configuration of the relative positions of multiple aircraft has great influence on the estimation error. When the distance information is combined with cooperative angle measurement of multiple aircraft [7], the relative distance between the multiple aircraft and the target cannot be estimated when they are collinear, and the estimation error is very large when they are approximately collinear. Therefore, the problem of detection configuration [7], [8], [12]–[14] should also be considered in the process of multi-interceptor guidance design.

In linear systems, the controller and estimator can be designed separately based on the separation theorem. In a previous study [8], a multi-model adaptive filter was added to the three-body cooperative guidance model to estimate and match the model of the incoming missile from an existing model set, and the defender intercepts the incoming missile in accordance with the model. In order to better track the maneuvering target, interactive multi-model filtering has also been incorporated in the design of a phased cooperative

guidance strategy of missiles [9]. The extended Kalman filter has also been used to estimate the target state [7], [12], [13], and optimal control, in combination with a linear kinematic model, is employed to constrain the interception angle of the endgame. All of the approaches discussed above use the separation theorem to design the controller and the estimator.

GST allows for the design of the estimator to be developed independently in the terminal guidance system. However, the probability density function (PDF) obtained by the estimator needs to be considered during the design of the guidance law [15] to [19]. The non-Gaussian PDF is calculated for the first time by using the multi-model state estimator introduced by [15]. The concept of model predictive control is used to propose the predictive control guidance law, which is then extended to the case of multiple targets. The concept of miss-set is proposed in [17], and the guidance law is proposed based on the design criterion of the optimal guidance law, in which the missile's miss-set contains the target's miss-set at all times. When compared with the techniques where the theory of differential game is used, the results show that the method has obvious advantages in performance. Building on the results of [15], the concept of the highest probability interval (HPI) was proposed by Dionne *et al.* [18]. HPI represents the regional value of the maximum probability of the missile intercepting the target. In [18], HPI is taken as the criterion to realize the design of the optimal guidance law of the missile, and the effectiveness of the method was verified by simulations. Compared with the conventional predictive guidance law, the method greatly improves the guidance performance as a smaller miss distance is obtained. Based on the results of [19], the study by [20] developed a more detailed optimal guidance law design scheme utilizing the HPI, and enhanced it to be capable of multi-target interception. On comparing the performance of optimal guidance law based on HPI and predictive guidance law, the results show that the former offers better performance and stronger adaptability for the purpose of intercepting multiple targets. While designing a many-to-many cooperative guidance law, [21] also used this idea to select a new performance index and verified the feasibility of this method through simulations.

In order to obtain more accurate target information and achieve better interception performance, it is necessary to measure or estimate other information beyond the line-of-sight (LOS) angle. Factors such as target acceleration, approach velocity, time-to-go and relative distance of the target can prove useful for this purpose. With the exception of the LOS angle and its rate of change, almost all of these factors depend on the measurement of the relative distance between the interceptors and the target. Therefore, the method of using multiple interceptors for cooperative measurement of relative distance has received extensive attention. In a previous study [22], the research objects were specified as two interceptors that could only measure LOS information. Based on interactive multiple model filtering and multiple model particle filter algorithms, real-time estimation of the

target motion is obtained using cooperative detection. While their results show that the cooperative detection method can significantly improve the interception performance, there is a requirement of improved real-time data processing. In the cooperative estimation of target motion information by multiple interceptors, the accuracy will be affected by the geometric configuration between the multiple interceptors and the target. In [7], the relative distance between the interceptors and the target was calculated by using the method of double line of sight measurement, which is also used as the input information for estimating the state of target motion. By increasing the LOS between the two interceptors and the target, the estimation accuracy of target motion information improves. On this basis, the cooperative guidance law of multiple aircraft was designed. On the basis of Liu *et al.* [7], Fonod and Shima [12], [13] further studied the influence of configuration on estimation accuracy and guidance performance. From the side of interceptors, [12] shows that applying different interception angles will affect the performance of estimation and guidance. When the interception angle between 30° and 65° is applied at the terminal of the guidance, better estimation and guidance performance can be generated for the target. Reference [13] established the research object as evader, and designed the "blind and evade" guidance law that can make the LOS angle of two interceptors consistent, which results in a decline in the estimation precision of the two interceptors. In order to allow for the evader to have a higher chance of survival, the evader was specified to adopt an escape strategy with bang-bang structure at the end.

The remainder of this paper is organized as follows: Section II, the cooperative interception engagement model is described, and the detection estimation error model is introduced. In Section III, the whole guidance process is categorized into unidentified and discriminated decoy stages. For the two stages, the predictive guidance law based on HPI and cooperative guidance law based on optimal control considering the detection configuration are designed respectively. In Section IV, the proposed guidance law is implemented in simulations, and the results are verified. The main findings of this paper are summarized in Section V.

II. PROBLEM STATEMENT

When an enemy's evader is engaged by our multi-pursuer, it could launch a decoy having similar characteristics in order to interfere with our pursuer. Our multiple pursuers need to identify the decoy and effectively target the enemy evader. The duration in the terminal guidance phase is very short, which is not advantageous as it needs take some time to identify the decoy. In addition, the relative guidance configuration of multiple pursuers will affect the detection accuracy of the evader during the cooperative guidance process. Therefore, in this work, we divide the final guidance law method into two stages: before and after identification of the decoy

The dynamic and kinematic models are established in the inertial coordinate system $X_I - O_I - Y_I$, as shown in Fig.1 is the planar engagement geometry of the evader and the two

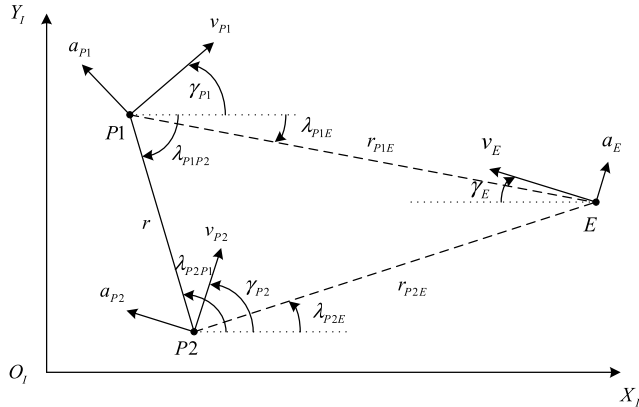


FIGURE 1. Planar engagement geometry.

pursuers. We denote the variables associated with the evader and pursuers by E and P_i respectively. The normal acceleration, speed, line-of-sight, range and flight-path angle are denoted by a , v , λ , r , and γ respectively.

A. KINEMATICS AND DYNAMICS

Neglecting the influence of gravity, the engagement process between the pursuer and the evader can be expressed in the form of polar coordinates (r, λ) as follows:

$$\dot{r}_{PiE} = v_{PiE} = -v_E \cos(\gamma_E - \lambda_{PiE}) - v_{Pi} \cos(\gamma_{Pi0} + \lambda_{PiE}); \quad i = \{1, 2\} \tag{1}$$

$$\dot{\lambda}_{PiE} = \frac{v_E \sin(\gamma_E - \lambda_{PiE}) - v_{Pi} \sin(\gamma_{Pi0} + \lambda_{PiE})}{r_{PiE}}; \quad i = \{1, 2\} \tag{2}$$

Above, \dot{r}_{PiE} is the relative velocity between the two aircraft, and λ_{PiE} is the LOS velocity between the two aircraft.

The normal acceleration of the aircraft, perpendicular to its motion (velocity), is a . During the entire guidance process, the speed of evader and pursuer is maintained constant. The relationship between the normal acceleration and flight-path angle of each aircraft can be obtained as:

$$\dot{\gamma}_i = \frac{a_i}{v_i}; \quad i = \{E, P_1, P_2\} \tag{3}$$

Remark 1: When the flight process of the two pursuers is approximately a nominal collision triangle, the above process can be linearized. In the engagement situation depicted in Fig.1, there are two collision triangles, formed between the evader and each of the pursuers.

After linearization, we can select the state vector as

$$\mathbf{x}_i = [x_1 \quad x_2 \quad x_3 \quad x_4]^T = \left[y_i \quad \frac{dy_i}{dt} \quad a_E \quad a_{Pi} \right]^T; \quad i = \{1, 2\} \tag{4}$$

$y_i \triangleq y_E - y_{Pi}$ is the lateral displacement between the decoy and the pursuer, and $\frac{dy_i}{dt}$ is the lateral relative velocity.

Assuming that pursuers and evader are approximately first-order dynamic models, the state equation of the relative

motion of the aircraft can be written as

$$\begin{cases} \dot{x}_1 = x_2 \\ \dot{x}_2 = x_3 - x_4 \\ \dot{x}_3 = \frac{a_E^c - x_3}{\tau_E} \\ \dot{x}_4 = \frac{a_{Pi}^c - x_4}{\tau_{Pi}} \end{cases}; \quad i = \{1, 2\} \tag{5}$$

Above, τ_{Pi} and τ_E is the actuation time constant of the pursuer P_i and evader E dynamics respectively.

The matrix form of the equation set (5) is

$$\dot{\mathbf{x}}_i = \mathbf{A}_i \mathbf{x}_i(t) + \mathbf{B}_i u_{Pi}(t) + \mathbf{C} a_E^c(t) + w(t); \quad i = \{1, 2\} \tag{6}$$

where,

$$\mathbf{A}_i = \begin{bmatrix} 0 & 1 & 0 & 0 \\ 0 & 0 & 1 & -1 \\ 0 & 0 & \frac{-1}{\tau_E} & 0 \\ 0 & 0 & 0 & \frac{-1}{\tau_{Pi}} \end{bmatrix}, \quad \mathbf{B}_i = \begin{bmatrix} 0 \\ 0 \\ 0 \\ \frac{1}{\tau_{Pi}} \end{bmatrix},$$

$$\mathbf{C} = \begin{bmatrix} 0 \\ 0 \\ \frac{1}{\tau_E} \\ 0 \end{bmatrix}$$

u_{Pi} is the control input for pursuer P_i , and satisfies the condition $|u_{Pi}| \leq u_{Pi}^{\max}$. a_E^c is the command acceleration of the evader E , and w is the noise in the guidance process.

After discretization of the linear system in equation (6), we get

$$\mathbf{x}_i(k+1) = \mathbf{F}_i \mathbf{x}_i(k) + \mathbf{G}_i u_{Pi}(k) + \mathbf{E}_i a_E^c(k) + w(k) \tag{7}$$

$$w(k) \sim N(0, \mathbf{Q}_w(k))$$

It is assumed that the simulation time interval of the discrete system is Δ . The matrices in equation (7) \mathbf{F}_i , \mathbf{G}_i , \mathbf{E}_i , and \mathbf{Q}_w are as follows:

$$\mathbf{F}_i = \Phi_i(\Delta) = \begin{bmatrix} 1 & \Delta & \tau_E(\Delta - \varphi_E) & -\tau_{Pi}(\Delta - \varphi_{Pi}) \\ 0 & 1 & \varphi_E & -\varphi_{Pi} \\ 0 & 0 & e^{-\Delta/\tau_E} & 0 \\ 0 & 0 & 0 & e^{-\Delta/\tau_{Pi}} \end{bmatrix} \tag{8}$$

$$\mathbf{G}_i = \int_0^\Delta \Phi_{Pi}(\Delta - \tau) \mathbf{B}_i d\tau = \begin{bmatrix} \tau_{Pi}(\Delta - \varphi_{Pi}) - \Delta^2/2 \\ \varphi_{Pi} - \Delta \\ 0 \\ 1 - e^{-\Delta/\tau_{Pi}} \end{bmatrix} \tag{9}$$

$$\mathbf{E}_i = \int_0^\Delta \Phi_{Pi}(\Delta - \tau) \mathbf{C} d\tau = \begin{bmatrix} -\tau_E(\Delta - \varphi_E) - \Delta^2/2 \\ -\varphi_E + \Delta \\ 1 - e^{-\Delta/\tau_E} \\ 0 \end{bmatrix} \tag{10}$$

$$\mathbf{Q}_w = \int_0^\Delta \Phi_{Pi}(\tau) \mathbf{Q} \Phi_{Pi}^T(\tau) d\tau \tag{11}$$

where, $\varphi_E = \tau_E(1 - e^{-\Delta/\tau_E})$, $\varphi_{P_i} = \tau_{P_i}(1 - e^{-\Delta/\tau_{P_i}})$, and \mathbf{Q} is a tuning matrix.

The initial range between the evader and the pursuers are denoted by $r_{P_1E_0}$ and $r_{P_2E_0}$. Under the assumption of that in the nominal collision triangle, the deviation between the flight-path angle γ_i and the LOS λ_{P_iE} is small. As a consequence, the time of interception of the pursuer to the evader is fixed:

$$t_{fP_iE} = \frac{-r_{P_iE_0}}{\dot{r}_{P_iE_0}} = \frac{r_{P_iE_0}}{v_E \cos(\gamma_{E_0} - \lambda_{P_iE_0}) + v_{P_i} \cos(\gamma_{P_{i0}} + \lambda_{P_iE_0})}; \quad i = \{1, 2\} \quad (12)$$

Remark 2: This paper considers the case where two pursuers intercept evaders at the same time such that the interception time of two pursuers to evaders is equal, i.e., $t_{fP_1E} = t_{fP_2E}$. Therefore, the range between two pursuers and evaders is specified to be also equal, $r_{P_1E_0} = r_{P_2E_0}$.

B. MEASUREMENT MODEL

Each pursuer measures LOS angle λ_{P_iE} using an IR sensor. In addition, each sensor is contaminated by the white gaussian noise v_{P_i} which is mutually independent during the measurement. We assume that the LOS angle measurement noise of each pursuer obeys the distribution

$$v_{P_i}^\lambda \sim N(0, \sigma_{P_i,\lambda}^2); \quad i = \{1, 2\} \quad (13)$$

It can be seen from Fig.1 that during the engagement a measurement baseline can be formed between the two pursuers relative to the evader. Assuming that the pursuers can accurately measure its relative state, and that the measurement information can be shared between the two pursuers, the relative position information $(r, \lambda_{P_iP_j})$, $i, j = 1, 2, i \neq j$ between them can be obtained

Therefore, the relative distance between the pursuers P_i and the evader E can be calculated through the known information that relative distance r between the pursuers and the LOS angle $\lambda_{P_iP_j}$ as follows:

$$\tilde{r}_{P_iE} = r \frac{\sin(\lambda_{P_iP_j} - \lambda_{P_jE})}{\sin(\lambda_{P_iE} - \lambda_{P_jE})} \quad (14)$$

where,

$$r = \sqrt{(x_{P_1} - x_{P_2})^2 + (y_{P_1} - y_{P_2})^2} \quad (15)$$

$$\lambda_{P_iP_j} = \arctan 2(y_{P_j} - y_{P_i}, x_{P_j} - x_{P_i}) \quad (16)$$

(x_{P_i}, y_{P_i}) and (x_{P_j}, y_{P_j}) in (15) and (16) can be obtained from the pursuer's respective equation of state, namely,

$$\dot{\mathbf{x}}_{P_i} = \mathbf{A}_{P_i}\mathbf{x}_{P_i} + \mathbf{B}_{P_i}u_{P_i} \quad (17)$$

where, the selected state vector is $\mathbf{x}_{P_i} = [y_{P_i} \ \dot{y}_{P_i} \ a_{P_i}]^T$;

$$\mathbf{A}_{P_i} = \begin{bmatrix} 0 & 1 & 0 \\ 0 & 0 & 1 \\ 0 & 0 & \frac{-1}{\tau_{P_i}} \end{bmatrix}, \mathbf{B}_{P_i} = \begin{bmatrix} 0 \\ 0 \\ \frac{1}{\tau_{P_i}} \end{bmatrix}.$$

Similarly, taking the state vector $\mathbf{x}_E = [y_E \ \dot{y}_E \ a_E]^T$, the equation of state of the evader can be obtained as

$$\dot{\mathbf{x}}_E = \mathbf{A}_E\mathbf{x}_E + \mathbf{B}_E a_E^c \quad (18)$$

where, $\mathbf{A}_E = \begin{bmatrix} 0 & 1 & 0 \\ 0 & 0 & 1 \\ 0 & 0 & \frac{-1}{\tau_E} \end{bmatrix}$, $\mathbf{B}_E = \begin{bmatrix} 0 \\ 0 \\ \frac{1}{\tau_E} \end{bmatrix}$, $a_E^c \leq a^{\max}$.

By using the assumption that linearization under the nominal collision triangle is satisfied, the lateral displacement y_i perpendicular to the initial LOS can be expressed as

$$y_i \approx (\lambda_{P_iE} - \lambda_{P_iE_0})r_{P_iE} \quad (19)$$

$$r_{P_iE} \approx v_{P_iE}t_{go} \quad (20)$$

where, t_{go} is defined as time-to-go of endgame,

$$t_{go} \triangleq \begin{cases} t_{fP_iE} - t, & t \leq t_{fP_iE} \\ 0, & t > t_{fP_iE}. \end{cases} \quad (21)$$

Combined with (14), the measurement equation of the pursuer can be obtained as

$$z_i = \mathbf{H}\mathbf{x}_i + v_{P_i}^y = y_i + v_{P_i}^y \quad (22)$$

where, $\mathbf{H} = [1 \ 0 \ 0 \ 0]$,

Remark 3: From the below (23) and (24), as shown at the bottom of this page, it can be seen that when the separation angle $|\lambda_{P_iE} - \lambda_{P_jE}|$ between the two pursuers and the evader decreases, the measurement variance of the lateral displacement y_i will increase, resulting in a decrease in the accuracy of state estimation. Therefore, in designing the guidance law, it is necessary to control the separation angle between the two pursuers and the evader at the appropriate stage.

III. DESIGN OF COOPERATIVE GUIDANCE

Here, we give a more detailed description of the engagement problem proposed in Section II where multi-pursuers can cooperatively intercept an enemy evader that is capable of launching a decoy. There are two main problems to be considered in the design of guidance law. First, in addition to a real target a false target with real target characteristics appears in the field of view of our pursuers after the evader launches the decoy. In this case, our aircraft needs to adopt an effective guidance method, which can take into account two

$$\sigma_{P_i,y} = \frac{r\lambda_{P_iE} \sqrt{\sin^2(\lambda_{P_iP_j} - \lambda_{P_iE})\sigma_{P_j,\lambda}^2 + \sin^2(\lambda_{P_iP_j} - \lambda_{P_jE})\cos^2(\lambda_{P_iE} - \lambda_{P_jE})\sigma_{P_i,\lambda}^2}}{\sin^2(\lambda_{P_iE} - \lambda_{P_jE})} \quad (23)$$

$$v_{P_i}^y \sim N(0, \sigma_{P_i,y}^2) \quad (24)$$

targets simultaneously and maximize the probability of intercepting the real target. Second, after identifying the decoy, the guidance configuration of the aircraft affects the detection accuracy of the target, i.e., the separation angle of the two pursuers affects the measurement variance of the lateral displacement. In this case, our pursuers need to control the separation angle of LOS at the guidance terminal such that it can meet the requirements of accuracy of detection and interception.

A. NO DECOYS IDENTIFIED

At this stage, we adopt a predictive control method which often called model predictive control (MPC), and it employs a receding horizon. The guidance problem has acceleration set as control input and miss distance as output error. The problem has two features: 1) The prediction horizon is the interception time, which varies with the future maneuvers and with the accuracy of the predicted missile and target states. 2) This method needs to estimate the target's state in real time and predict its state at the time of interception. The guidance law based on GST takes into account the PDF output of the estimator, denoted as $p(z_E | y^k)$.

For a single target, although the maneuvering form is difficult to predict, the PDF output by the estimator can be approximately considered to be normally distributed. For the special situation of target releasing decoy, the PDF output by the estimator may be multimodal. At this point, it may be assumed that the PDF output by the estimator is a summation of one or more PDFs subject to normal distribution. It can be assumed that these PDFs subject to normal distribution correspond to the state estimation of each target and decoy. In Fig.2, the flow diagram of the predictive guidance law is shown.

The guidance control problem at this stage mainly involves two aspects. One is the transition from the state at moment t_k , solved by the receding control constraint, to the prediction state at the interception time t_f . The other is to solve the piecewise-constant optimal controller while satisfying the receding control constraints within the receding time interval $[t_k, t_{k+1}]$. The main idea of the guidance law design at this stage is to maximize the probability density of the target in the reachable set of the interceptor; this is shown in Fig.3

1) CALCULATION OF THE RECEDING CONTROL CONSTRAINT

The receding control constraint is obtained by maximizing the probability of the target's state in the pursuer's reachable set. Let $R_{Pi}(t_f, t_{k+1})$ be the set of states reachable by the pursuer at time instant t_f , given that the state was $x_{Pi}(t_{k+1})$ at time instant t_{k+1} . In addition, let $\beta_{Pi}(t_f, t_{k+1})$ be the set of positions reachable by the pursuer at time instant t_f provided the state was $x_{Pi}(t_{k+1})$ at time instant t_{k+1} , that is

$$\beta_{Pi}(t_f, t_{k+1}) \triangleq D_\beta R_{Pi}(t_f, t_{k+1}) \\ = [\beta_{Pi}^{\min}(t_f, t_{k+1}), \beta_{Pi}^{\max}(t_f, t_{k+1})] \quad (25)$$

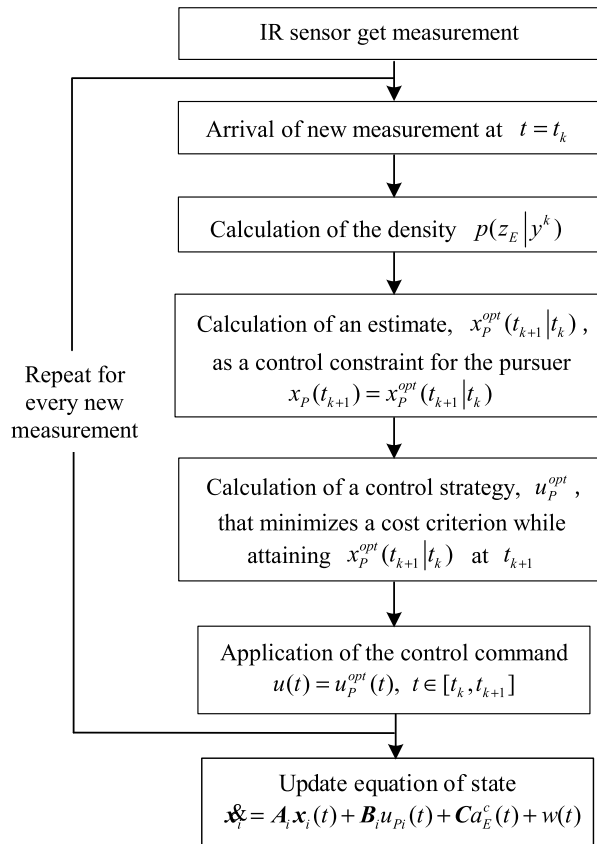


FIGURE 2. Flow diagram of the proposed predictive guidance law.

Above, $D_\beta = [1 \ 0 \ 0]$. Assume $\bar{\beta}_{Pi}(t_f, t_{k+1})$ is a subinterval of $\beta_{Pi}(t_f, t_{k+1})$ that can be expressed as

$$\bar{\beta}_{Pi}(t_f, t_{k+1}) \triangleq [\beta_{Pi}^{\min}(t_f, t_{k+1}) + \theta(t_f, t_{k+1}), \\ \beta_{Pi}^{\max}(t_f, t_{k+1}) - \theta(t_f, t_{k+1})] \quad (26)$$

where $\beta_{Pi}^{\min}(t_f, t_{k+1})$ and $\beta_{Pi}^{\max}(t_f, t_{k+1})$ are the upper and lower limits of the state that the pursuer can reach from time t_k to time t_f subject to the condition of the maximum command acceleration. $\theta(t_f, t_{k+1})$ is the maximum displacement of the peak of the probability density function of target state from time t_{k+1} to time t_f .

As can be seen in Fig.3, the required receding control constraint condition is

$$x_{Pi}(t_{k+1}) = x_{Pi}^{opt}(t_{k+1} | t_k) \quad (27)$$

where, $x_{Pi}^{opt}(t_k | t_{k+1})$ satisfies the optimization problem

$$x_{Pi}^{opt}(t_k | t_{k+1}) = \arg \max_{x_{Pi}(t_{k+1} | t_k) \in R} U(x_{Pi}(t_{k+1} | t_k)) \quad (28)$$

$$U(x_{Pi}(t_{k+1} | t_k)) \triangleq \int_{\beta_{Pi}(t_f, t_{k+1})} p(z_E | y^k) dz_E \quad (29)$$

Here, U is the probability that the target is in the reachable set at time t_{k+1} .

In Fig.3, the control input $u(\tau)$, $\tau \in [t_k, t_{k+1}]$ can make the state $x_{Pi}(t_k)$ reach different values $x_{Pi}(t_{k+1})$ within the range

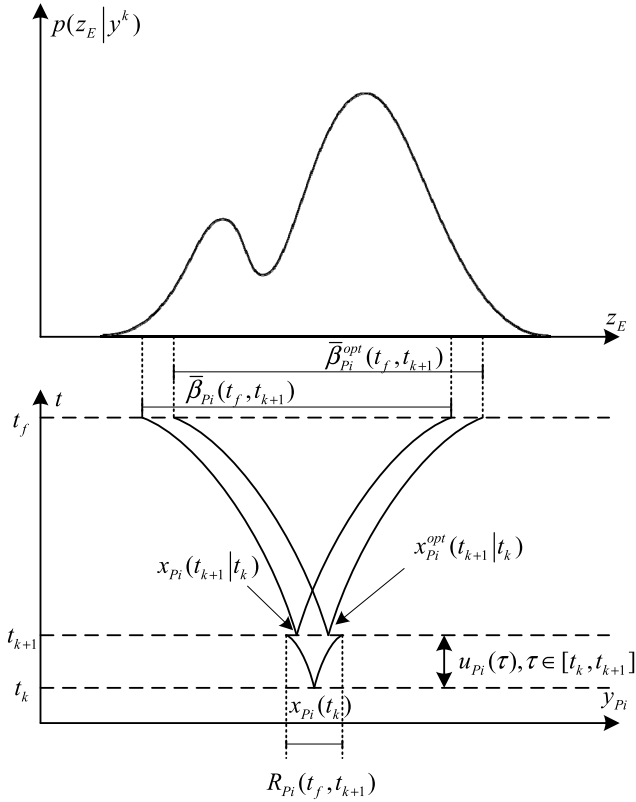


FIGURE 3. Receding horizon optimization.

of reachable set at the next moment t_{k+1} ; the optimal solution $\mathbf{x}_{P_i}^{opt}(t_{k+1} | t_k)$ can maximize the probability U that the target is in the reachable set at time t_{k+1} .

Remark 4: An approximate method to solve the optimal solution can be obtained. From a number of reachable sets $\bar{\beta}_{P_i}(t_f, t_{k+1})$ with different state values $\mathbf{x}_{P_i}(t_{k+1})$ as the center starting point, the interval that can make the probability U reach the maximum is found. This interval is also called the highest probability interval (HPI), and the corresponding central starting point is the optimal solution $\mathbf{x}_{P_i}^{opt}(t_{k+1} | t_k)$.

2) CALCULATION OF THE CONTROL COMMAND

When solving for the control command $u(\tau)$, $\tau \in [t_k, t_{k+1}]$, it is necessary to calculate the control command $u(\tau)$ in each time interval $[t_k, t_{k+1}]$. Therefore, in the whole guidance process, the control command $u(\tau)$ is a piecewise-constant function composed of many control commands in the subinterval $[t_k, t_{k+1}]$.

A performance index $J^{OL}(t_k)$ related to the piecewise control command $u(\tau)$ can be expressed as:

$$J^{OL}(t_k) \triangleq \left| z_{P_i}^{HPI}(t_k) - z(t_{k+1} | t_k) \right| \tag{30}$$

$$z_{P_i}^{HPI}(t_k) \triangleq \mathbf{D}_\beta \Phi_{P_i}(t_f, t_{k+1}) \mathbf{x}_{P_i}^{opt}(t_{k+1} | t_k) \tag{31}$$

$$\begin{aligned} z(t_{k+1} | t_k) &\triangleq \mathbf{D}_\beta \Phi_{P_i}(t_f, t_{k+1}) \mathbf{x}_{P_i}(t_{k+1} | t_k) \\ &= \mathbf{D}_\beta (\Phi_{P_i}(t_f, t_k) \mathbf{x}_{P_i}(t_k) \\ &\quad + \int_{t_k}^{t_{k+1}} \Phi_{P_i}(t_f, \tau) \mathbf{B}_{P_i}(\tau) u^{OL}(\tau) d\tau) \end{aligned} \tag{32}$$

In the above, $z_{P_i}^{HPI}(t_k)$ and $z(t_{k+1} | t_k)$ are the projection of the position given by the state $\mathbf{x}_{P_i}^{opt}(t_{k+1} | t_k)$ and $\mathbf{x}_{P_i}(t_{k+1} | t_k)$ from time t_{k+1} to time t_f .

From equations (30) to (32), only the function $z(t_{k+1} | t_k)$, related to the control command $u(\tau)$, is known. In addition, we don't need to calculate $\mathbf{x}_{P_i}^{opt}(t_{k+1} | t_k)$ to get $z_{P_i}^{HPI}(t_k)$. As $z_{P_i}^{HPI}(t_k)$ is the projection point of $\mathbf{x}_{P_i}^{opt}(t_{k+1} | t_k)$ at time t_f , it is the center point of the HPI; hence, we can get $z_{P_i}^{HPI}(t_k)$ by simply calculating the HPI at time t_f .

In order to solve the performance index $J^{OL}(t_k)$, Theorem III.1 is introduced, and we set $g(t_k) = z_{P_i}^{HPI}$ and $f(t_{k+1}) = \mathbf{D}_\beta \Phi_{P_i}(t_f, t_{k+1})$.

Theorem 1: Consider a linear system with state variables $\mathbf{x}_{P_i}(\tau) \in \mathbf{R}$, transition matrix Φ_{P_i} , control input $u^{OL}(\tau) \in \mathbf{R}$, and input matrix \mathbf{B}_{P_i} . Now we look at the following control problem:

$$\inf_{u^{OL} \in A_u} |g(t_k) - f(t_{k+1}) \mathbf{x}_{P_i}(t_{k+1})| \tag{33}$$

$$A_u \triangleq \left\{ \left| u^{OL}(\tau) \right| \leq u_{P_i}^{max}, \tau \in [t_k, t_{k+1}] \right\} \tag{34}$$

where, only $\mathbf{x}_{P_i}(t_{k+1})$ is the function related with the control input $u^{OL}(\tau) \in [t_k, t_{k+1}]$.

Define the function

$$\xi(\tau) \triangleq f(t_{k+1}) \Phi_{P_i}(t_{k+1}, \tau) \mathbf{B}_{P_i}(\tau), \quad \tau \in [t_k, t_{k+1}] \tag{35}$$

Assuming Φ_{P_i} and \mathbf{B}_{P_i} are matrices that are continuous in time, $\xi(\tau)$ is not equal to zero and does not change sign. Then, there is an optimal control command $u^{OL}(\tau) = u_d^*(t_k)$, $\tau \in [t_k, t_{k+1}]$ satisfying $u^{OL} \in A_u$ in each time interval $[t_k, t_{k+1}]$ to make (33) reach the optimal condition.

Therefore, the optimal control command can be obtained as

$$u_d^*(t_k) = \begin{cases} K(t_k) / \zeta(t_k), & |K(t_k) / \zeta(t_k)| \leq u_{P_i}^{max} \\ u_{P_i}^{max} \text{sgn}(K(t_k) / \zeta(t_k)), & \text{otherwise} \end{cases} \tag{36}$$

where,

$$K(t_k) \triangleq g(t_k) - f(t_{k+1}) \Phi(t_{k+1}, t_k) \mathbf{x}_{P_i}(t_k) \tag{37}$$

$$\zeta(t_k) \triangleq \int_{t_k}^{t_{k+1}} \xi(\tau) d\tau \tag{38}$$

Proof: Assuming that the value of (33) is equal to a constant c , we get

$$\begin{aligned} c &= \inf_{u^{OL} \in A_u} \left| K(t_k) + \rho(u^{OL}) \right|, \\ \rho(u^{OL}) &\triangleq - \int_{t_k}^{t_{k+1}} \xi(\tau) u^{OL}(\tau) d\tau \end{aligned} \tag{39}$$

Case 1: Assume $c \neq 0$. Due to the uncertainty of the $u^{OL}(\tau)$, we have

$$c = \min \left\{ \left| K(t_k) + \rho^{min} \right|, \left| K(t_k) + \rho^{max} \right| \right\} \tag{40}$$

where,

$$\rho^{min} \triangleq \inf_{u^{OL} \in A_u} \rho(u^{OL}), \quad \rho^{max} \triangleq \sup_{u^{OL} \in A_u} \rho(u^{OL}) \tag{41}$$

By virtue of the assumption that $\xi(\tau)$ is not equal to zero and does not change the sign all the way through, we can get

$$\rho^{\min} = -u^{\max} \left| \int_{t_k}^{t_{k+1}} \xi(\tau) d\tau \right| = -u^{\max} |\zeta(t_k)| \quad (42)$$

$$\rho^{\max} = u^{\max} \left| \int_{t_k}^{t_{k+1}} \xi(\tau) d\tau \right| = u^{\max} |\zeta(t_k)| \quad (43)$$

Consequently, when $K(t_k) > 0$ and $c \neq 0$, we can get the infimum of c as $c = |K(t_k) + \rho^{\min}|$. According to (39), the optimal control input can be obtained as

$$u^{OL}(\tau) = \begin{cases} u^{\max} & \text{if } \zeta(t_k) > 0 \\ -u^{\max} & \text{if } \zeta(t_k) < 0 \end{cases} \\ \tau \in [t_k, t_{k+1}], \quad \text{if } c \neq 0, K(t_k) > 0 \quad (44)$$

When $K(t_k) < 0$ and $c \neq 0$, we can the infimum of c as $c = |K(t_k) + \rho^{\max}|$. Then, the optimal control input can be obtained as

$$u^{OL}(\tau) = \begin{cases} -u^{\max} & \text{if } \zeta(t_k) > 0 \\ u^{\max} & \text{if } \zeta(t_k) < 0 \end{cases} \\ \tau \in [t_k, t_{k+1}], \quad \text{if } c \neq 0, K(t_k) < 0 \quad (45)$$

Therefore, the optimal control input can be expressed as

$$u_d^*(t_k) = u^{\max} \text{sgn}(K(t_k)/\zeta(t_k)) \quad (46)$$

Case 2: Assume $c = 0$. Then we have

$$\inf_{u^{OL} \in A_u} |K(t_k) + \rho(u^{OL})| = 0 \quad (47)$$

As $\rho(u^{OL}) \triangleq - \int_{t_k}^{t_{k+1}} \xi(\tau) u^{OL}(\tau) d\tau$, and $\xi(\tau)$ is not equal to zero, the optimal control input can be obtained as

$$u_d^*(t_k) = K(t_k) / \left(\int_{t_k}^{t_{k+1}} \xi(\tau) d\tau \right) = K(t_k) / \zeta(t_k) \quad (48)$$

Hence, it can be proved that the optimal control command is given by equation (36).

3) APPLICATION TO MODEL

Using (25), the reachable set of position components in the state vector of the linear system in equation (17) can be obtained as:

$$\beta_{P_i}^{\min} = \mathbf{D}_\beta (\Phi_{P_i}(t_f, t_k) \mathbf{x}_{P_i}(t_k) - u_{P_i}^{\max} \int_{t_k}^{t_f} \Phi_{P_i}(t_f, \tau) \mathbf{B}_{P_i} d\tau) \quad (49)$$

$$\beta_{P_i}^{\max} = \mathbf{D}_\beta (\Phi_{P_i}(t_f, t_k) \mathbf{x}_{P_i}(t_k) + u_{P_i}^{\max} \int_{t_k}^{t_f} \Phi_{P_i}(t_f, \tau) \mathbf{B}_{P_i} d\tau) \quad (50)$$

The target randomly launches a decoy with similar characteristics to the target within the time interval $\tau \in [0, t_f]$ for the interception by the pursuer, and applies the maximum reverse command acceleration to interfere with the pursuer. Therefore, the pursuer has two similar targets in the field of view. PDFs of two similar target states can be calculated by the Kalman filter. Before the decoy is launched, the PDF

of the target state follows the Gaussian distribution. After the decoy is launched, the PDF of the target state can be approximated as the sum of the M Gaussian densities with equal probability. At any given time, the value of M is

$$M(t_k) = 1 + N_d(t_k) \quad (51)$$

where N_d is the number of unidentified decoys.

The maximum change of the peak value of the probability density function of the target position from time t_k to time t_f is θ . The estimated value of state $\hat{\mathbf{X}}_k$ and variance $P_{k|k} \in R^{5 \times 5}$ of (6) can be obtained through Kalman filtering. Assuming that the pursuer's lateral displacement y_{P_i} , lateral velocity \dot{y}_{P_i} , and command acceleration u_{P_i} are known, the current estimated state value $\hat{\mathbf{X}}_k^{AT}$ of the target can be expressed as $[y_{P_i} + \hat{\mathbf{X}}_k(1) \quad \dot{y}_{P_i} + \hat{\mathbf{X}}_k(2) \quad \hat{\mathbf{X}}_k(3)]^T$. The current estimated value of variance can be expressed as

$$P_{k|k}^{AT} = I_{3 \times 5} P_{k|k} I_{3 \times 5}^T, \quad I_{3 \times 5} \triangleq [I_{3 \times 3} \quad |0_{3 \times 2}|] \quad (52)$$

where $I_{3 \times 3}$ is the identity matrix.

Using the values of the current mean and variance of the target state, and combining the kinematic equation of the target, the mean and variance of the position in the target state at the terminal moment t_f can be obtained, as given below

$$\hat{\mathbf{X}}_p^{AT}(t_f) = \mathbf{D}_\beta \Phi_E(t_f, t_k) \hat{\mathbf{X}}_k^{AT} \quad (53)$$

$$P_p^{AT}(t_f | t_k) = \mathbf{D}_\beta \Phi_{P_i}(t_f, t_k) P_{k|k}^{AT} \Phi_{P_i}^T(t_f, t_k) \mathbf{D}_\beta^T \quad (54)$$

θ is composed of two parts - θ_1 and θ_2 . θ_1 is the change in value of the target position from time t_k to time t_f under the maximum command acceleration, and θ_2 is the standard deviation of the estimated value of position in the target state.

$$\theta(t_k) = \theta_1(t_k) + \alpha \theta_2(t_k) \quad (55)$$

$$\theta_1(t_k) \triangleq a^{\max} D_E \int_{t_k}^{t_f} \Phi_E(t_f, \tau) \mathbf{B}_E d\tau \\ = a^{\max} \left(\frac{t_{go}^2}{2} - \tau_E t_{go} + \tau_E^2 (1 - e^{-t_{go}/\tau_E}) \right) \quad (56)$$

$$\theta_2(t_k) \triangleq \sqrt{P_p^{AT}(t_f | t_k)} = \sqrt{\mathbf{D}_\beta \Phi_{P_i}(t_f, t_k) P_{k|k}^{AT} \Phi_{P_i}^T(t_f, t_k) \mathbf{D}_\beta^T} \quad (57)$$

Using (36), the optimal solution for the linear system in (17) while obeying the condition of (30) can be given by the following two equations:

$$K(t_k) = z_{P_i}^{HPI}(t_k) - \left(y_{P_i}(t_k) + \dot{y}_{P_i}(t_k) t_{go} + a_{P_i}(t_k) \right. \\ \left. \times \left[\tau_{P_i} t_{go} + \tau_{P_i}^2 (e^{-t_{go}/\tau_{P_i}} - 1) \right] \right) \quad (58)$$

$$\zeta(t_k) = \Delta(t_{go} - \tau_{P_i}) + \tau_{P_i}^2 e^{-t_{go}/\tau_{P_i}} (e^{\Delta/\tau_{P_i}} - 1) - \frac{\Delta^2}{2} \quad (59)$$

B. BDECOYS IDENTIFIED

When the decoy is identified, if the guidance law designed in Section III.A is adopted continuously, the separation angle of the two pursuers may become smaller as the predictive

guidance law cannot control the LOS angle. According to Remark 3, in this case, the accuracy of state estimation will become worse. After the decoy is identified, if the pursuer with a large initial LOS angle maximizes its LOS angle and the other one minimizes its LOS angle, then the separation LOS angle of the two pursuers will become larger and the estimation accuracy will be enhanced.

Therefore, an optimal control approach will be adopted in this stage to achieve the conditions discussed above by taking miss distance and energy consumption into consideration.

1) COST FUNCTION

Assuming small deviation under the nominal collision triangle condition, the lateral displacement of the pursuer can be approximated as

$$y_i \approx (\lambda_{PiE} - \lambda_{PiE_0})r_{PiE} \quad (60)$$

$$r_{PiE} \approx v_{PiE}t_{go} \quad (61)$$

Then, LOS angle λ_{PiE} can be approximated as

$$\lambda_{PiE} \approx \lambda_{PiE_0} + \frac{y_i}{v_{PiE}t_{go}} \quad (62)$$

Therefore, the term $\frac{y_i}{t_{go}}$ is introduced and the performance index of the optimal control is set as

$$J^y = \frac{1}{2}ay_i^2(t_f) + \frac{1}{2}b \int_{t_k}^{t_f} u_{Pi}^2 d\tau + \frac{1}{2}c \int_{t_k}^{t_f} \frac{y_i(t_f)}{t_{go} + \Delta t} d\tau \quad (63)$$

where $\Delta t > 0$, is a small quantity close to zero.

Remark 5: We use $\frac{y_i(t_f)}{t_{go} + \Delta t}$ instead of $\frac{y_i(t_f)}{t_{go}}$ to avoid a singularity in the following derivation. When $\Delta t \rightarrow 0$, $\frac{y_i(t_f)}{t_{go} + \Delta t} \rightarrow \frac{y_i(t_f)}{t_{go}}$. Letting $a \rightarrow \infty$ yields a perfect guidance law. Note here that if the weight $c > 0$, the LOS angle is minimized, and the LOS angle is maximized when $c < 0$.

2) ORDER REDUCTION

In order to reduce the order of solving the optimization problem and to obtain an analytical solution for the control input, the terminal projection method [23] is introduced. This requires us to introduce new state variables $Z_i(t)$, defined as follows:

$$Z_i(t) = \mathbf{D}\Phi_i(t_f, t)\mathbf{x}_i(t) \quad (64)$$

where $\Phi_i(t_f, t)$ is the state transition matrix related to (6), \mathbf{D} is constant vector used to separate elements in the state variables $\mathbf{x}_i(t)$. For instance, when $\mathbf{D} = [1 \ 0 \ 0 \ 0]$, we can separately retrieve the lateral displacement y_i from the state vector \mathbf{x}_i . We also have

$$\dot{\Phi}_i(t_f, t) = -\Phi_i(t_f, t)\mathbf{A}_i \quad (65)$$

Combining (65) with the time derivative of the new state variable, we can obtain

$$\begin{aligned} \dot{Z}_i(t) &= \mathbf{D}\dot{\Phi}_i(t_f, t)\mathbf{x}_i(t) + \mathbf{D}\Phi_i(t_f, t)\dot{\mathbf{x}}_i(t) \\ &= \mathbf{D}\Phi_i(t_f, t)\mathbf{B}_i u_{Pi}(t) \end{aligned} \quad (66)$$

Equation (66) indicates that $\dot{Z}_i(t)$ is state independent and only related to the designed controller, and $\mathbf{D}\Phi_i(t_f, t)\mathbf{B}_i$ is denoted as \hat{B}_i .

Using the terminal projection method to reduce the order, the objective function of (63) can be expressed as

$$J^Z = \frac{1}{2}aZ_i^2(t_f) + \frac{1}{2}b \int_{t_k}^{t_f} u_{Pi}^2 d\tau + \frac{1}{2}c \int_{t_k}^{t_f} \frac{Z_i(t_f)}{t_{go} + \Delta t} d\tau \quad (67)$$

3) OPTIMAL CONTROLLER

The Hamiltonian function of the performance index is

$$H = \frac{1}{2}bu_{Pi}^2 + \frac{1}{2}c \frac{Z_i(t)}{t_{go}} + \lambda_Z \dot{Z}_i(t) \quad (68)$$

The time derivatives of the new state variables are state independent, simplifying considerably the adjoint equations

$$\dot{\lambda}_Z = -\frac{\partial H}{\partial Z_i} = -\frac{c}{2t_{go}} \quad (69)$$

$$\lambda_Z(t_f) = aZ_i(t_f) \quad (70)$$

Integrating (69) from t_0 to t_f , and substituting (70) in it, we get

$$\lambda_Z(t) = aZ_i(t_f) + \frac{1}{2}c \ln \frac{t_{go}}{\Delta t} \quad (71)$$

From the control equation, we can get

$$\begin{aligned} \frac{\partial H}{\partial u_{Pi}} &= 0 \\ \Rightarrow u_{Pi} &= -\frac{\hat{B}_i}{b} \left[aZ_i(t_f) + \frac{c}{2} \ln \frac{t_{go}}{\Delta t} \right] \end{aligned} \quad (72)$$

Substituting (72) into (66), we have

$$\dot{Z}_i(t) = -\frac{\hat{B}_i^2}{b} aZ_i(t_f) - \frac{c\hat{B}_i^2}{2b} \ln \frac{t_{go}}{\Delta t} \quad (73)$$

Integrating (73) from t_0 to t_f , we have

$$Z_i(t_f) - Z_i(t) = -\frac{a}{b} Z_i(t_f) \hat{B}_{i1} - \frac{c}{2b} \hat{B}_{i2} \quad (74)$$

where $\hat{B}_{i1} = \int_t^{t_f} \hat{B}_i^2 d\tau$, $\hat{B}_{i2} = \int_t^{t_f} \hat{B}_i^2 \ln \frac{t_{go}}{\Delta t} d\tau$.

The $Z_i(t_f)$ is solved as

$$Z_i(t_f) = \frac{Z_i(t) - \frac{c}{2b} \hat{B}_{i2}}{1 + \frac{a}{b} \hat{B}_{i1}} \quad (75)$$

Substituting $Z_i(t_f)$ into (72), and the optimal controller is obtained as

$$u_{Pi} = -\hat{B}_i \left[\frac{Z_i(t) - \frac{c}{2b} \hat{B}_{i2}}{\frac{a}{b} + \hat{B}_{i1}} + \frac{c}{2} \ln \frac{t_{go}}{\Delta t} \right] \quad (76)$$

Letting $a \rightarrow \infty$, we can get a perfect intercept guidance law, i.e

$$u_{Pi} = -\hat{B}_i \left[\frac{Z_i(t) - \frac{c}{2b} \hat{B}_{i2}}{\hat{B}_{i1}} + \frac{c}{2} \ln \frac{t_{go}}{\Delta t} \right] \quad (77)$$

IV. SIMULATION ANALYSIS

In this section, numerical simulation is used to analyze the proposed phased guidance law. First, we set the simulation parameters and analyze the engagement of the four aircraft. We then use Monte Carlo (MC) simulations to evaluate the estimated accuracy and guidance performance of the pursuer on the proposed phased guidance law; these results are compared with the pure predictive guidance methods based on HPI and augmented proportional navigation (APN) based on minimum mean square error (MMSE), both of which are proposed by Dionne et al. [20]. The difference between HPI and MMSE lies in the processing of target (including decoy) state. HPI fully considers PDF of target state, while MMSE only performs simple processing.

A. INTERCEPTION SCENARIO AND PARAMETERS

For the guidance law designed for Section III, the following simulation parameters are set: Pursuer 1 and pursuer 2 are both launched at the same time, and the initial range from the evader is $r_{PiE_0} = 10000$ m. The initial lateral separation are $y_{P1E_0} = -400$ m and $y_{P2E_0} = -300$ m. The speed of the pursuer and the evader is $v_{Pi} = 700$ m/s and $v_E = 300$ m/s. Neglecting the effect of gravity, the maximum command acceleration for the pursuer and evader is $a_{Pi}^{max} = 15$ g and $a_E^{max} = 3$ g; the pursuer's and evader's actuation time constants are $\tau_{Pi} = 0.2$ s and $\tau_E = 0.2$ s. The measurement simulation time interval is $\Delta = 0.01$ s, and the standard deviation of LOS angle measurement noise is $\sigma_{Pi,\lambda} = 0.1$ mrad. The decoy employs the reverse maximum acceleration command with $a_D^{max} = 3$ g.

In order to realize MC simulation, the initial condition of filtering is sampled from a Gaussian distribution:

$$\hat{x}_{i_0} \sim N(x_{i_0}, P_0) \tag{78}$$

where, x_{i_0} is the true initial state defined by equation (4). P_0 is the initial covariance matrix of the filter,

$$P_0 = \text{diag}\{50^2, 10^2, 1^2, 10^2\} \tag{79}$$

Fig.4 shows the engagement trajectories between the evader, pursuer1, pursuer2, and decoy. The evader fires a decoy at 2s to interfere with the pursuers. If the discrimination delay of the decoy is 3s, the pursuer can only identify the real target after 5s. According to the guidance law designed in Section III, before the deployment of the decoy, the pursuer adopts the guidance law in Section III.A, which can take two targets into account at the same time. Following the deployment of the decoy, the pursuer adopts the guidance law in Section III.B, which can control the separation angle of LOS.

Fig.5 shows the change of lateral displacement of the evader with respect to pursuer 1 and pursuer 2. The lateral separation of pursuer1 and pursuer2 with respect to evader is seen to change from around 400 m and 300 m to zero respectively. However, after the evader launches a decoy to distract the pursuers, the lateral separation between pursuers and evader within the discrimination delay of 3 s becomes

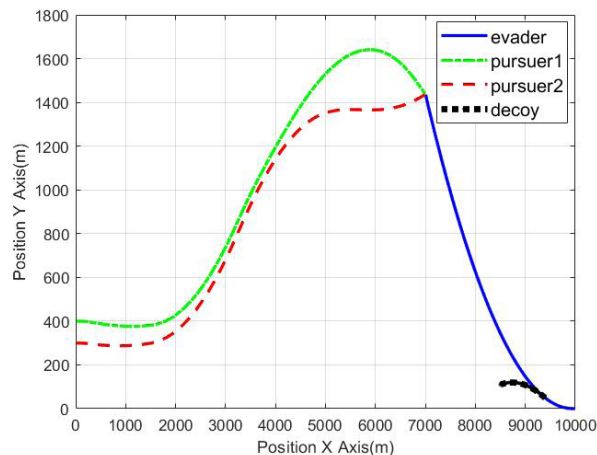


FIGURE 4. Multi-aircraft cooperative interception engagement trajectories with a decoy whose deployed and discriminated time are 2s and 5s.

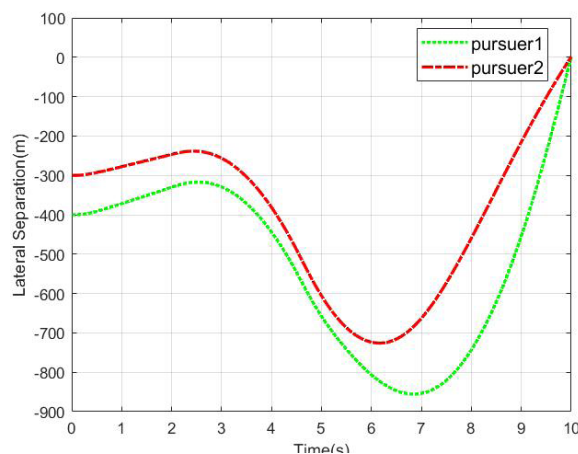


FIGURE 5. Lateral separation of pursuer1 and pursuer2 whose initial separation are -400 m and -300 m.

larger gradually. Until the decoy is identified, pursuer 1 and pursuer 2 use the guidance law in Section III.B, and the lateral separation between them and the evader begins to decrease until zero.

In Fig.6, we plot the acceleration profiles of the evader, pursuer1 and pursuer2. While subject to the limit of maximum acceleration command $u_{Pi}^{max} = 15$, the change in the acceleration of pursuer 1 and pursuer 2 is basically the same for the first 5 seconds. After the launch of the decoy, their acceleration changed dramatically and reached the limit value soon. It should be noted that the acceleration trends of pursuer 1 and pursuer 2 are different before and after 5 s because of the different guidance laws adopted.

B. ESTIMATION PERFORMANCE EVALUATION

In Fig.7, we show a variation curve of the lateral separation measurement noise between pursuer1 and the evader for different guidance laws. Fig.8 shows the variation curve of LOS separation angle between the two pursuers when using differ-

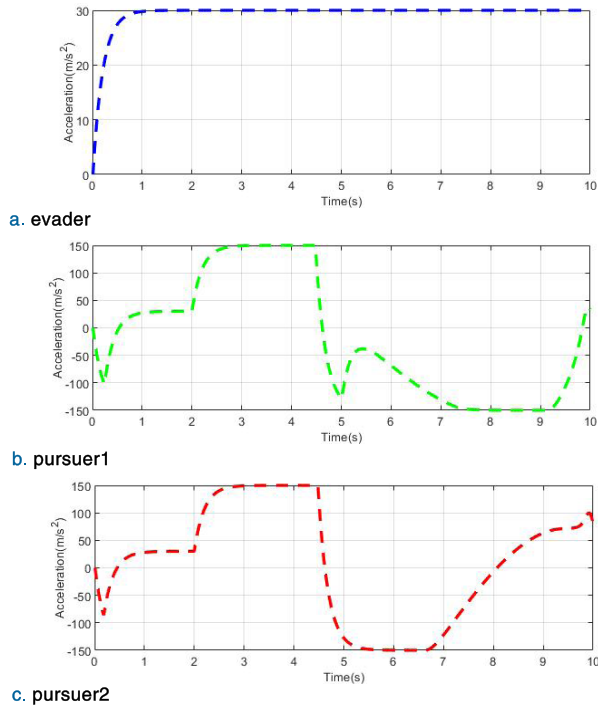


FIGURE 6. Acceleration profiles of evader, pursuer1, and pursuer2 whose maximum value are 3g, 15g, and 15g. The pursuer1 and pursuer2 switch guidance law at 5s.

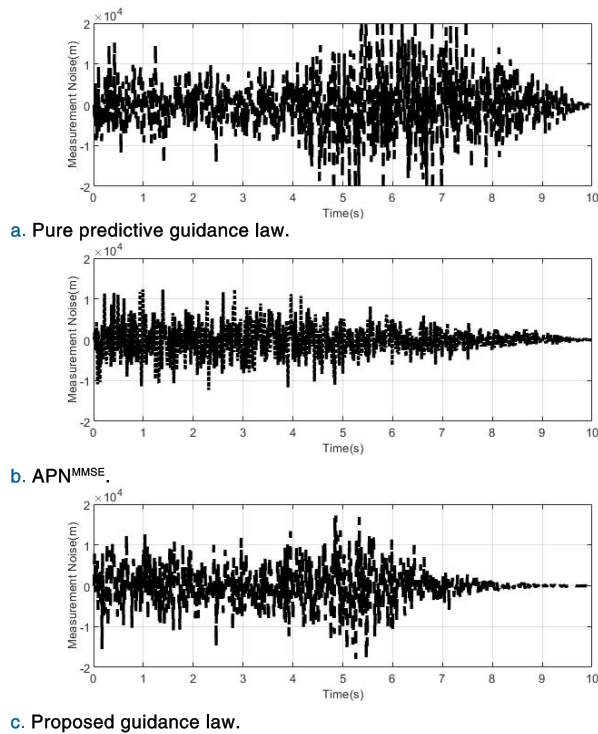


FIGURE 7. Measurement noise of pursuer1 in the pure predictive guidance law, APN MMSE and the proposed guidance law.

ent methods. It can be seen the two figures that, before 5 s, the separation angle of LOS is small, and that makes their lateral separation detection error larger. This is because the predictive guidance based on HPI and APN guidance law

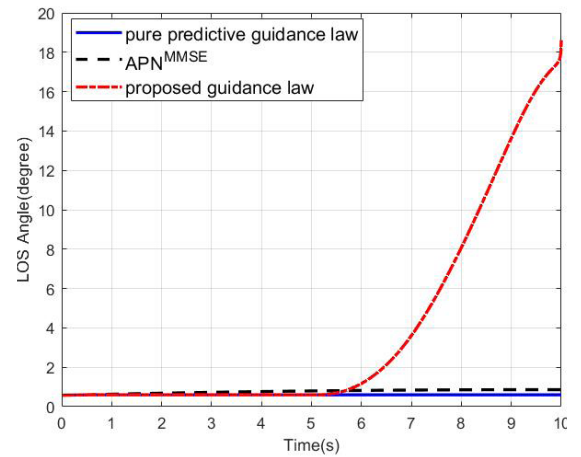


FIGURE 8. LOS separation angle of pursuer1 in the pure predictive guidance law, APN^{MMSE}, and the proposed guidance law.

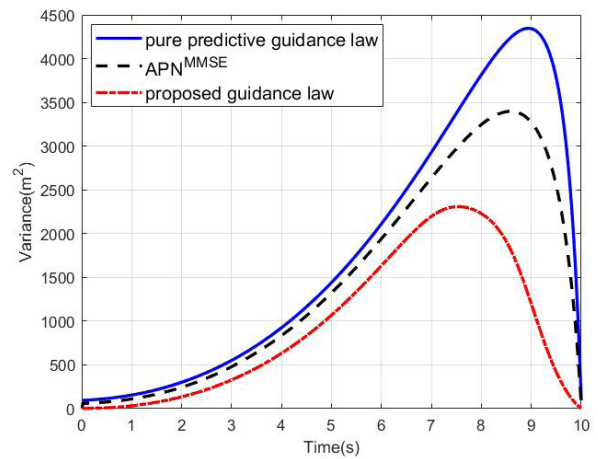


FIGURE 9. Variance of state estimation errors of pursuer1 evaluated based on 500 MC runs in the pure predictive guidance law, APN^{MMSE}, and the proposed guidance law.

based on MMSE (APN^{MMSE}) cannot control the LOS angle between pursuers and evader. After 5 s, the separation angle of LOS based on pure predictive guidance law and APN^{MMSE} is still small, but the proposed guidance law that can control the separation angle of LOS and make it larger than before. The measurement noise becomes smaller with the increase of the separation angle of LOS and finally reaches near zero. Thus, the proposed guidance law can decrease the detection error for the pursuer.

Fig.9 show the variance of state estimation error through 500 MC simulations. The variance increases with time at first before gradually decreasing. The variance in the case where the pure predictive guidance law was used is seen to be larger. In addition, the proposed guidance law can make the variance of state estimation finally approach to zero, which meets our requirements for estimation accuracy. However, it is to be noted that the pure predictive guidance law and APN^{MMSE} cannot ensure the variance decrease to zero, which can yield the detection error.

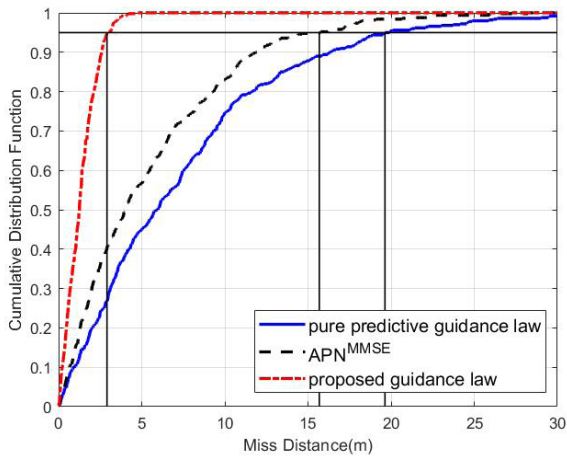


FIGURE 10. Miss distance cumulative distribution function of pursuer1 in the pure predictive guidance law, APN^{MMSE}, and the proposed guidance law.

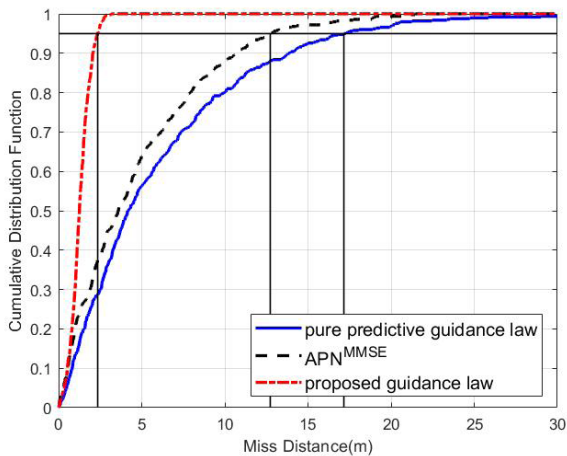


FIGURE 11. Miss distance cumulative distribution function of pursuer2 in the pure predictive guidance law, APN^{MMSE}, and the proposed guidance law.

C. MISS DISTANCE EVALUATION

Here, we analyze the closed-loop interception performance of the pure predictive guidance law, APN^{MMSE}, and the proposed guidance law through 500 MC simulations.

Fig.10 and Fig.11 present the miss distance cumulative distribution function (CDF) of the pursuer1 and pursuer2, which is defined by the minimum of the miss distances of pursuers. The required warhead lethality ranges (WLR) to ensure a 95% kill probability as summarized in TABLE 1 Taking pursuer1 as an example, the required WLR of the proposed guidance law is 2.91 m compared to 19.63 m required WLR of pure predictive guidance law and 15.68 m required WLR of APN^{MMSE} at the condition of ensuring a 95% kill probability respectively As can be seen from the Fig.10 and Fig.11, the required WLR of the proposed guidance law is much lower than the pure predictive guidance law and APN^{MMSE}. The results show that the interception

TABLE 1. Required warhead lethality ranges of pure predictive guidance law, APn^{MMSE}, and proposed guidance law to ensure a 95% kill probability.

Guidance law	Pursuer1, m	Pursuer2, m
Pure predictive guidance law	19.63	17.16
APN ^{MMSE}	15.68	12.73
Proposed guidance law	2.91	2.35

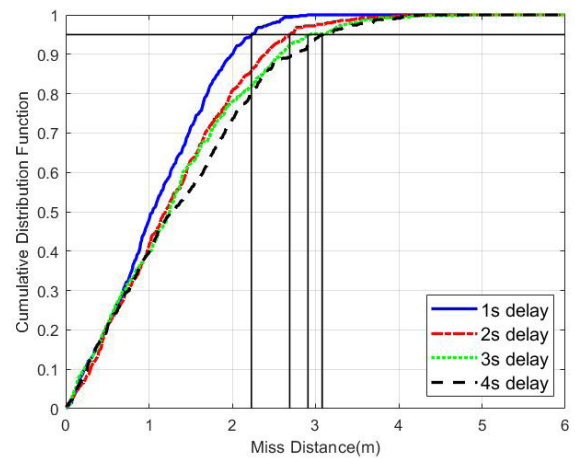


FIGURE 12. Miss distance cumulative distribution function of different unidentified delay in the proposed guidance law.

TABLE 2. Required warhead lethality ranges of proposed guidance law with different unidentified delay to ensure a 95% kill probability.

Guidance law	1s delay, m	2s delay, m	3s delay, m	4s delay, m
Proposed guidance law	2.23	2.69	2.91	3.08

performance of the proposed guidance law is better than the pure predictive guidance law and APN^{MMSE}.

Taking pursuer1 as example, Fig.12 present the miss distance distribution function for different unidentified delay. The required WLR of the proposed guidance law with different unidentified delay to ensure a 95% kill probability are summarized in TABLE 2. The required WLR of the proposed guidance law with 1s, 2s, 3s, and 4s unidentified delay are 2.23 m, 2.69 m, 2.91 m, and 3.08 m respectively. As can be seen from Fig.12, with the increase of unidentified delay, the pursuer needs to get the required WLR much more. This illustrates that the short unidentified delay can reduce the miss distance and strength guidance accuracy.

V. CONCLUSION

This paper proposes the use of a phased cooperative guidance law to handle scenarios in which an enemy evader deploys a decoy in response to engagement by two pursuers. During the unidentified decoy stage, a predictive guidance law based on HPI is employed. An optimal guidance law, which takes into

account detection of the geometric configurations, is used in the discriminated decoy stage.

For the first stage, due to the existence of the unidentified decoy, the PDF of the targets is multimodal and is composed of the state of the real target and false target. Therefore, we use the predictive guidance law introducing the concept of the GST to design the controller, which account for the real target and the false target at the same time in guidance process This approach provides the interception maneuver advantage for the later cooperative guidance towards the real target. For the second stage when the decoy is discriminated, we use a guidance law based on optimal control to increase the LOS separation angel between the pursuers and the target to reduce the estimation error and to improve the guidance accuracy.

Using MC simulations, we compare the performance between the proposed guidance law, APN^{MMSE} , and the pure predictive guidance law The results indicate that the proposed model has a lower estimation error and higher guidance accuracy than the pure predictive guidance law and APN^{MMSE} . In addition, a short discriminated delay can improve the interception performance, and hence, it is necessary to design a fast and effective detector

REFERENCES

- [1] T. Shima, "Optimal cooperative pursuit and evasion strategies against a homing missile," *J. Guid., Control, Dyn.*, vol. 34, no. 2, pp. 414–425, Mar. 2011, doi: [10.2514/1.51765](https://doi.org/10.2514/1.51765).
- [2] M. Sayadi, A. Kosari, and P. M. Zadeh, "Robust optimal control for precision improvement of guided gliding vehicle positioning," *IEEE Access*, vol. 6, pp. 25797–25815, 2018, doi: [10.1109/ACCESS.2018.2810204](https://doi.org/10.1109/ACCESS.2018.2810204).
- [3] A. Perelman, T. Shima, and I. Rusnak, "Cooperative differential games strategies for active aircraft protection from a homing missile," *J. Guid., Control, Dyn.*, vol. 34, no. 3, pp. 761–773, May 2011, doi: [10.2514/1.51611](https://doi.org/10.2514/1.51611).
- [4] T. Shima, "Intercept-angle guidance," *J. Guid., Control, Dyn.*, vol. 34, no. 2, pp. 484–492, Mar. 2011, doi: [10.2514/1.51026](https://doi.org/10.2514/1.51026).
- [5] R. E. Kalman, "A new approach to linear filtering and prediction problems," *J. Basic Eng.*, vol. 82, no. 1, pp. 35–45, Mar. 1960, doi: [10.1115/1.3662552](https://doi.org/10.1115/1.3662552).
- [6] R. E. Kalman and R. S. Bucy, "New results in linear filtering and prediction theory," *J. Basic Eng.*, vol. 83, no. 1, pp. 95–108, Mar. 1961, doi: [10.1115/1.3658902](https://doi.org/10.1115/1.3658902).
- [7] Y. Liu, N. Qi, and J. Shan, "Cooperative interception with double-line-of-sight-measuring," in *Proc. AIAA Guid., Navigat., Control (GNC) Conf.*, Boston, MA, USA, Aug. 2013, pp. 2013–5112, doi: [10.2514/6.2013-5112](https://doi.org/10.2514/6.2013-5112).
- [8] V. Shaferman and T. Shima, "Cooperative multiple-model adaptive guidance for an aircraft defending missile," *J. Guid., Control, Dyn.*, vol. 33, no. 6, pp. 1801–1813, Nov. 2010, doi: [10.2514/1.49515](https://doi.org/10.2514/1.49515).
- [9] V. Shaferman and Y. Oshman, "Stochastic cooperative interception using information sharing based on engagement staggering," *J. Guid., Control, Dyn.*, vol. 39, no. 9, pp. 2127–2141, Sep. 2016, doi: [10.2514/1.G000437](https://doi.org/10.2514/1.G000437).
- [10] W. M. Wonham, "On the separation theorem of stochastic control," *SIAM J. Control*, vol. 6, no. 2, pp. 312–326, May 1968.
- [11] H. S. Witsenhausen, "Separation of estimation and control for discrete time systems," *Proc. IEEE*, vol. 59, no. 11, pp. 1557–1566, Nov. 1971, doi: [10.1109/PROC.1971.8488](https://doi.org/10.1109/PROC.1971.8488).
- [12] R. Fonod and T. Shima, "Estimation enhancement by cooperatively imposing relative intercept angles," *J. Guid., Control, Dyn.*, vol. 40, no. 7, pp. 1711–1725, Jul. 2017, doi: [10.2514/1.G002379](https://doi.org/10.2514/1.G002379).
- [13] R. Fonod and T. Shima, "Blinding guidance against missiles sharing bearings-only measurements," *IEEE Trans. Aerosp. Electron. Syst.*, vol. 54, no. 1, pp. 205–216, Feb. 2018, doi: [10.1109/TAES.2017.2747098](https://doi.org/10.1109/TAES.2017.2747098).
- [14] S. Zhang, Y. Guo, and S. Wang, "Cooperative intercept guidance of multiple aircraft with a lure role included," *Int. J. Aerosp. Eng.*, vol. 2018, pp. 1–15, Apr. 2018.
- [15] R. A. Best and J. P. Norton, "Predictive missile guidance," *J. Guid., Control, Dyn.*, vol. 23, no. 3, pp. 539–546, May 2000, doi: [10.2514/2.4562](https://doi.org/10.2514/2.4562).
- [16] I. G. Shaviv and Y. Oshman, "Fusion of estimation and guidance using sequential Monte Carlo methods," in *Proc. IEEE Conf. Control Appl. CCA.*, Piscataway, NJ, USA, Aug. 2005, pp. 1361–1366, doi: [10.1109/CCA.2005.1507321](https://doi.org/10.1109/CCA.2005.1507321).
- [17] I. Shaviv and Y. Oshman, "Guidance without assuming separation," in *Proc. AIAA Guid., Navigat., Control Conf. Exhibit*, San Francisco, CA, USA, Aug. 2005, pp. 2005–6154, doi: [10.2514/6.2005-6154](https://doi.org/10.2514/6.2005-6154).
- [18] D. Dionne, H. Michalska, and C. A. Rabbath, "A predictive guidance law with uncertain information about the target state," in *Proc. Amer. Control Conf.*, Piscataway, NJ, USA, Jun. 2006, p. 6, doi: [10.1109/ACC.2006.1656357](https://doi.org/10.1109/ACC.2006.1656357).
- [19] D. Dionne and C. Rabbath, "Predictive guidance for pursuit-evasion engagements involving decoys," in *Proc. AIAA Guid., Navigat., Control Conf. Exhibit*, Keystone, CO, USA, Aug. 2006, pp. 2006–6214, doi: [10.2514/6.2006-6214](https://doi.org/10.2514/6.2006-6214).
- [20] D. Dionne, H. Michalska, and C. A. Rabbath, "Predictive guidance for pursuit-evasion engagements involving multiple decoys," *J. Guid., Control, Dyn.*, vol. 30, no. 5, pp. 1277–1286, Sep. 2007, doi: [10.2514/1.25481](https://doi.org/10.2514/1.25481).
- [21] B. Yang, H. H. T. Liu, and Y. Yao, "Cooperative interception guidance for multiple vehicles: A receding horizon optimization approach," in *Proc. IEEE Chin. Guid., Navigat. Control Conf.*, Aug. 2014, pp. 827–831, doi: [10.1109/cgnc.2014.7007317](https://doi.org/10.1109/cgnc.2014.7007317).
- [22] V. Shaferman and Y. Oshman, "Cooperative interception in a multi-missile engagement," in *Proc. AIAA Guid., Navigat., Control Conf.*, Chicago, IL, USA, Aug. 2009, pp. 2009–5783, doi: [10.2514/6.2009-5783](https://doi.org/10.2514/6.2009-5783).
- [23] E. A. Bryson and C. Y. Ho, *Applied Optimal Control*. Waltham, MA, USA: Blaisdell, 1969, pp. 154–155, 282–289.



SHAOBO WANG received the B.S. degree from the Taiyuan University of Technology, China, in 2018. He is currently pursuing the M.S. degree in control science and engineering with the Xi'an Research Institute of High-Technology. His current research interests include optimal control and flight control.



YANG GUO received the M.S. and Ph.D. degrees in guidance, navigation, and control and the Ph.D. degree in control science and engineering from the Xi'an Research Institute of High-Technology, Xi'an, China, in 2008 and 2012, respectively. He is currently an Associate Professor with the Xi'an Research Institute of High-Technology. His research interests include finite-time control and flight control.



SHICHENG WANG received the B.S., M.S., and Ph.D. degrees in automatic control from the Xi'an Research Institute of High-Technology, China, in 1985, 1988, and 1992, respectively. He is currently a Professor with the Xi'an Research Institute of High-Technology. His research interest includes flight vehicle guidance and simulation.



SHUAI ZHANG received the B.S. and M.S. degrees from the Xi'an Research Institute of High-Technology, China, in 2013 and 2016, respectively, where he is currently pursuing the Ph.D. degree in control science and engineering. His current research interests include optimal control, finite-time control, and flight control.

...



ZHIGUO LIU received the master's and Ph.D. degrees in control science and engineering from the Xi'an Research Institute of High-Technology, China, in 2003 and 2008, respectively. He is currently an Associate Professor with the Xi'an Research Institute of High-Technology. His research interests include precision guidance and simulation, and control theory and engineering.